Lee Kuan Yew School of Public Policy

Asia Competitiveness Institute

ACI Research Paper #14-2021

Impact of Travel Bubbles:

Cooperative Travel Arrangements in a Pandemic

Taojun XIE

Jiao WANG

Shiqi LIU

July 2021

Please cite this article as:

Xie, Taojun, Jiao Wang and Shiqi Liu, "Impact of Travel Bubbles: Cooperative Travel Arrangements in a Pandemic," Research Paper #14-2021, *Asia Competitiveness Institute Research Paper Series (July 2021)*

Impact of Travel Bubbles: Cooperative Travel Arrangements in a Pandemic*

Taojun Xie† Jiao Wang‡ Shiqi Liu§

July 1, 2021

Abstract

We develop a two-region Susceptible-Infected-Recovered-Macroeconomic model to evaluate the cooperative and non-cooperative cross-border travel arrangements during a pandemic. In a symmetric setting, the Pareto optimal is a cooperative travel arrangement that emphasizes exclusively on domestic containment. A non-cooperative game between social planners results in high travel restrictions with little benefit in economics or health. With asymmetric pandemic dynamics, a border closure on average results in less welfare loss than a non-cooperative game, compared to cooperation. A border control allowing minimal essential travel only delays the outbreak in a region initially not infected. This can however be remedied by a timely vaccination plan. Under cooperation, pre-departure tests further enhance the welfare. Applying our model, we estimate that the Singapore – Hong Kong travel bubble is valued at US$635.1 per capita, and the Australia – New Zealand travel bubble is valued at US$307.8 per capita.

*We thank colleagues at Asia Competitiveness Institute for constructive comments. Declarations of interest: none.

†Asia Competitiveness Institute, Lee Kuan Yew School of Public Policy, National University of Singapore. Email: tjxie@nus.edu.sg.

‡Melbourne Institute: Applied Economic & Social Research, Faculty of Business and Economics, The University of Melbourne. Email: jiao.wang@unimelb.edu.au.

§Asia Competitiveness Institute, Lee Kuan Yew School of Public Policy, National University of Singapore. Email: E0000928@u.nus.edu.

1 Introduction

The prevalence of travel restrictions due to the coronavirus 2019 (COVID-19) pandemic almost brought the global travel industry to a complete stop. Realizing that such travel restrictions were no longer sustainable as the pandemic extended into year 2021, policy makers started contemplating ways to reopen the borders. Some actively look for allies to plan on resuming bilateral or regional travel. Others wait to see how their counterparts move. Although it has been unanimously agreed that opening the borders is key to reviving the economies, the fear of recurrences of health crises has lead to some policy makers holding back. What are the benefits of regions cooperating on cross-border travel? What are the externalities of one region's holding-back on its potential partners? This paper aims to provide answers.

Broadly, existing travel arrangements can be categorized into cooperative and non-cooperative ones. Policy makers from two or more regions sometimes cooperate, allowing residents in these regions to travel across the borders in a less restrictive, if not free, way. Green lanes were established in a few Asian regions to expedite the clearance for business travel. "Travel bubbles" have also been negotiated between Singapore and Hong Kong, and between Australia and New Zealand, with the objective to facilitate easier travel for non-essential purposes. Some regions, however, prefer not to cooperate. At one extreme, policy makers adopt a *lazzie-faire* approach, with no travel restrictions imposed. In some cases, limited availability of air tickets, long periods of quarantine on arrival, and mandatory medical tests are major hurdles for travelers as policy makers struggle to contain the pandemic at home while preventing imported infection. It is also not unusual that some decide to completely shut down the borders, or to exercise border controls, allowing only essential travel. The heterogeneous approaches to resuming cross-border travel are results of the difficulty in evaluating the health-economics tradeoff, calling for an analytical framework capable of identifying the optimal policy action.

We provide such an analytical framework to formally assess the implications of the above-mentioned cross-border travel arrangements for economics, health, and societal welfare. To do so, we construct a two-region Susceptible-Infected-Recovered-Macroeconomic (SIR-Macro) model and look for the Ramsey solutions to social planners' problems. Our model is based on Eichenbaum et al. (2021), henceforth ERT, a workhorse framework for analyzing macroeconomic issues in a pandemic. This model assumes people make economic decisions based on both economic and health factors. Krueger et al. (2020) (henceforth KUX) further extend it to multiple sectors. We depart from ERT and KUX by allowing people to travel between regions subject to travel restrictions. This extension introduces two important sources of health risks which policy makers are most wary of. First, while traveling abroad, interacting with local people places one at risk of infection if there are infected people in the destination region. Second, while not traveling, interacting with travelers coming from the other region also entails a risk of getting infected. Understanding the health-economics tradeoff, and the existence of negative externalities, the social planners in our model derive optimal domestic containment and travel restrictions to achieve highest joint or domestic welfare, according to their decision to cooperate or not.

As the key contribution of the paper, we provide a framework for evaluating a wide range of travel arrangements in a pandemic. The challenges in evaluating such travel arrangements arise from the facts that there are more than one policy makers at stake, leading to possible prisoners' dilemma, and that the costs and benefits of cross-border travel in a pandemic need to be carefully calculated when designing the policies. Our framework addresses both challenges. To our best knowledge, we are the first to derive optimal travel-related policies in both cooperative and non-cooperative settings. Based on this framework, we assess the values of existing and upcoming travel arrangements between Singapore and Hong Kong, and between Australia and New Zealand. The results of these assessments provide useful bases in inter-region discussions pertaining to reopening the borders.

Several key findings emerge in the paper. First, optimal cooperative policy is the best policy response. Cooperation in the two regions leads to global welfare gain compared to the open-loop Nash (non-cooperative) equilibrium in which each policy maker only maximizes its own social welfare. The cooperative equilibrium shows a heavy emphasis on domestic containment while in the non-cooperative regime, social planners rely on high restrictions to cross-border travel. Moreover, initial infection conditions matter for the size of the gain. Cooperation is more beneficial to the region where the pandemic originates from.

Second, among the border management policies, border control induces much higher costs than border closure does in a region not initially infected. In fighting against the pandemic, border management policies have been commonly adopted by policy makers. The costs are largely born by the region without the initial pandemic, because failure to completely shut down the border, i.e. a border control that allows minimal essential travel, only delays a domestic infection outbreak transmitted from the infected region. One remedy for the delayed infection due to border control is a timely vaccination plan. Our simulations show that vaccinating the population in the no-pandemic region within two years offsets the welfare loss due to border control and domestic containment is gradually lifted towards the end of the vaccination plan.

Third, our results show that pre-departure tests are welfare improving only when regions cooperate. As policy makers are wary of imported infection, pre-departure tests are nowadays commonplace for identifying infected travelers and preventing the pandemic from spreading across the border. Such a measure, however, does not always lead to better welfare outcome. The benefits of pre-departure tests are practically zero at the non-cooperative equilibrium. This is because while travel restrictions are relaxed with pre-departure tests, domestic containment is stricter as infected people consume and interact more domestically. Domestic consumption is lower, offsetting the benefit of partial recovery in travel consumption.

Last but not the least, we calibrate our model to a couple of real-world cooperative travel arrangements between Singapore and Hong Kong, and between Australia and New Zealand. These arrangements are commonly known as "travel bubbles". Taking into account country-specific features, our simulation results show that on average having a travel bubble arrangement, i.e. optimal cooperative equilibrium, leads to a welfare gain valued at US$635.1 per capita for Singapore – Hong Kong and one valued at US$307.8 per capita for Australia – New

Zealand. Individually, the travel bubble is more beneficial to New Zealand than to Australia. It is due to the fact that travel consumption carries a larger weight in the consumption basket of the New Zealand residents who benefit more from a lesser restriction under the cooperative travel arrangement. This result highlights the important role of a country's travel openness in influencing the value of travel bubbles.

Our paper is related to two strands of literature. First, it joins the fast-expanding literature on COVID-19-related policy discussions. There are papers with closed-economy settings, such as Eichenbaum et al. (2021); Krueger et al. (2020); Acemoglu et al. (2020); Alvarez et al. (2020); Brotherhood et al. (2020); Glover et al. (2020); Guerrieri et al. (2020), among others. There are also papers dealing with open economies such as Giannone et al. (2020); Hou et al. (2021); George et al. (2021); Hsu et al. (2020). Most of the open-economy literature, however, either focuses on the economic spillover effects of a pandemic via trade linkages, or on the spread of the pandemic via human movements. The impact on an economy due to the movements of people is usually overlooked, let along policies designed to balance the economic and health tradeoff. We fill the gap by explicitly modeling the transmission of economic impact due to cross-border human flows, and deriving optimal policies for targeting at both domestic economic activity and cross-border travel.

In addition, it relates to the literature on optimal policy in open economies. The majority of this literature focuses on optimal monetary policy in a two-country setting, including Obstfeld and Rogoff (1995, 2002); Corsetti and Pesenti (2001, 2005); Clarida et al. (2002); Benigno and Benigno (2006); Engel (2011); among others. Some have an additional focus on policy games of cooperation and noncooperation under optimal monetary policy, such as Bodenstein et al. (2019); Fujiwara and Wang (2017). We adopt the optimal policy games of this literature and apply them to examine optimal containment policies between regions in a pandemic.

The remainder of the paper is organized as follows. Section 2 describes the model. Section 3 shows the baseline simulation results and Section 4 shows results with asymmetric pandemic development. Vaccination and testings are examined in Section 5. The model is then applied to two examples of travel bubbles in Section 6 and Section 7 concludes.

2 Model

Our model is based on the SIR-Macro framework of ERT. The SIR-Macro framework has been the workhorse model for studies on the macroeconomic issues of a pandemic. In normal time with no pandemic, the model resembles a neo-classical macroeconomic model. At the onset of a pandemic, a fraction of the population gets infected. The rest of the population then face the risk of getting infected when interacting with the infected people through economic activity. The probability of dying from infection is taken into account in people's lifetime utility. Those who are not yet infected therefore may wish to reduce interactions with the infected people to ensure better health, but at the cost of lower utility from consumption.

We extend the SIR-Macro framework to a two-region setting and introduce travel-related policies. People in each region may consume within their geographical boundary, or travel to the

other region. In normal time with no pandemic, the model is similar to one with internationally traded goods. During the pandemic, since traveling between the regions involves movements of people, pandemic in one region is spread to another region. From residents' point of view, the risk of cross-border infection needs to be taken into account in their economic decisions. Travel consumption is substituted by domestic consumption if the pandemic is more severe in the other region. And from the social planner's point of view, policies that control the cross-border movements of travelers may be useful tools in containing the pandemic in the region. Our model therefore introduces such policies and analyze their effectiveness.

As our objective is to provide a framework for analyses of travel arrangements, we make a few simplifications for the ease of explaining the key mechanism. Firstly, as in KUX, we assume a perfectly mobile labor market in each region. This is because the performance of the travel industry relies largely on people's consumption preference rather than on the labor market. The supply of travel-related goods, hence the labor supply, then adjusts to meet the market demand. We also abstract the infection via the labor market from the model so that the policies discussed focus on infection via travelers. Secondly, we do not discuss the role of exchange rate across the regions. Although it is true that some travel arrangements indeed are discussed between regions using different currencies, the focus is still on reviving the real economy. We therefore abstract exchange rate dynamics from the model and consider only the real variables. Nonetheless, we acknowledge that the labor market dynamics and the role of exchange rate are important areas for future research.

2.1 Normal time

The model consists of two regions, H and F. Consumption bundle of a representative agent in any region consists of non-travel-related domestic consumption goods and travel-related consumption goods in the other region. Both regions have the same set of variables. Although it suffices to list the equations for just one of the regions, it is useful to note that, in general, we denote the variables of residents in F with asterisks. In the case of consumption goods, where the origins matter, we use a subscript H to denote goods produced in region H, and a subscript F to denote goods produced in region F. The consumption bundle for an agent in H is written as

$$C_t = \left[(1-\upsilon)^{1/\eta} C_{Ht}^{1-1/\eta} + \upsilon^{1/\eta} C_{Ft}^{1-1/\eta}\right]^{\frac{\eta}{\eta-1}}$$

where C_t is the aggregate consumption, C_{Ht} is the spending on domestic consumption goods, and C_{Ft} is the travel spending in region F. The parameter $\upsilon \in (0,1)$ is the share of travel spending in F by residents of H during normal time, which we interpret as the travel openness. $\eta > 0$ is the elasticity of substitution across different spending categories. The period utility of the agent is

$$u(C_t, N_t) = \log C_t - \frac{\theta}{2} {N_t}^2$$

where N_t is the labor supply and $\theta > 0$ is a parameter governing the disutility in labor. The budget constraint is

$$(1+\rho_t) P_t C_{Ht} + (1+\rho_t^*)(1+\mu_t^*) P_t^* C_{Ft} = W_t N_t + \Gamma_t$$

where P_t and P_t^* are price levels in H and F respectively, W_t is the wage rate and Γ_t is government rebates. ρ_t and ρ_t^* are consumption taxes imposed in H and F respectively. μ_t^* denotes the travel restrictions imposed in F. Government budget is balanced, such that all proceeds from consumption and travel taxes are rebated to the residents:

$$\Gamma_t = \rho_t C_{Ht} + (\rho_t + \mu_t + \rho_t \mu_t) C_{Ht}^*$$

Note that μ_t denotes the travel restrictions imposed in H and C_{Ht}^* is the travel-related spending of an agent from F in region H. Firms produce outputs with linear production technology A to meet demands from both regions

$$C_{Ht} + C_{Ht}^* + \Gamma_t = A N_t$$

Wage is normalized to unity for all regions, $W_t = 1$. Prices are competitive and equal to marginal cost $P_t = \frac{1}{A}$.

2.2 Pandemic

At the onset of a pandemic, people are distinguished according to their health status. In total, there are four types. A susceptible person (s) has not been infected and are subject to an infection risk. Once infected, a susceptible person is identified as an infected person (i), who subsequently recovers (r) or dies (d). Both an infected person and a recovered person are immune to the pandemic. They will not be infected for the second time. The population sizes of the four types of people are denoted by S_t, I_t, R_t, and D_t. Their respective shares in the pre-pandemic population are $\hat{S}_t$, $\hat{I}_t$, $\hat{R}_t$ and $\hat{D}_t$. For a type-j person who is alive, the consumption bundle is

$$C_t{}^j = \left[(1-\upsilon)^{1/\eta} C_{Ht}^j{}^{1-1/\eta} + \upsilon^{1/\eta} C_{Ft}^j{}^{1-1/\eta} \right]^{\frac{\eta}{\eta-1}}$$

for $j \in \{s, i, r\}$. In what follows, we describe the optimization problem for different agent types. Utility for a deceased person is assumed to be zero, i.e $U_t^d = 0$.

Recovered A recovered person behaves in the same way as a representative agent during normal time. This is because she is immune and does not get infected again. Accordingly, she maximizes her lifetime utility

$$U_t^r = u(C_t^r, N_t^r) + \beta E_t U_{t+1}^r;$$

subject to the budget constraint. β is the discount factor. The first-order conditions with respect to domestic and travel consumption and labor supply are

$$C^r_{Ht}: \quad (1+\rho_t)\,\lambda^r_{bt} = (1-\upsilon)^{1/\eta}\left(\frac{C^r_{Ht}}{C^r_t}\right)^{-1/\eta}\frac{1}{C^r_t} \tag{1}$$

$$C^r_{Ft}: \quad (1+\rho^*_t)\,(1+\mu^*_t)\,\lambda^r_{bt} = \upsilon^{1/\eta}\left(\frac{C^r_{Ft}}{C^r_t}\right)^{-1/\eta}\frac{1}{C^r_t} \tag{2}$$

$$N^r_t: \quad \theta N^r_t = A\lambda^r_{bt} \tag{3}$$

where λ^r_{bt} is the Lagrange multiplier associated with the budget constraint. Solving for $\lambda^r_{b,t}$ from Eq. (3) and substituting into Eqs. (1) and (2), one obtains

$$\theta N^r_t = (1-\upsilon)^{1/\eta}\left(\frac{C^r_{Ht}}{C^r_t}\right)^{-1/\eta}\frac{A}{C^r_t}\frac{1}{1+\rho_t}$$

$$\theta N^r_t = \upsilon^{1/\eta}\left(\frac{C^r_{Ft}}{C^r_t}\right)^{-1/\eta}\frac{A}{C^r_t}\frac{1}{1+\mu^*_t}\frac{1}{1+\rho^*_t}$$

Solutions for C^r_{Ht} and C^r_{Ft} are obtained by taking the ratio of the above two equations and substituting into the CES consumption aggregator

$$C^r_{Ht} = \frac{(1-\upsilon)\,(1+\rho_t)^{-\eta}\,C^r_t}{\Lambda_t}$$

$$C^r_{Ft} = \frac{\upsilon\,(1+\rho^*_t)^{-\eta}\,(1+\mu^*_t)^{-\eta}\,C^r_t}{\Lambda_t}$$

where $\Lambda_t \equiv \left[(1-\upsilon)\,(1+\rho_t)^{1-\eta} + \upsilon\,(1+\rho^*_t)^{1-\eta}\,(1+\mu^*_t)^{1-\eta}\right]^{\frac{\eta}{\eta-1}}$. For $\eta > 1$, exorbitantly strict containment measures in region F result in little travel from H to F, in other words, $\lim_{\mu^*_t\to\infty} C^r_{Ft} = 0$. Substitute the solutions into the respective first-order conditions and we have

$$\theta N^r_t = \frac{A}{C^r_t}\Lambda_t^{1/\eta}$$

From the budget constraint,

$$\Lambda_t^{-1/\eta} C^r_t = AN^r_t + A\Gamma_t$$

Rearranging the above two equations,

$$\frac{A}{\theta N^r_t} = AN^r_t + A\Gamma_t$$

where Γ_t are proceeds from the containment measures and travel restrictions. Without any policy in either region, Γ_t is zero, and N^r_t and C^r_t are constant.

Infected An infected agent has $\pi_r \in [0,1]$ probability of recovery in the following period, and $\pi_d \in [0,1]$ probability of dying of the disease. She maximizes lifetime utility expressed as the following bellman equation

$$U_t^i = u\left(C_t^i, N_t^i\right) + \beta E_t\left[\pi_r U_{t+1}^r + (1-\pi_r-\pi_d)U_{t+1}^i\right]$$

subject to the budget constraint. The first-order conditions are identical to a recovered agent's. Without containment measures or travel restrictions, consumption and travel spending of an infected agent are constant.

This behavior of infected people creates negative externalities. The infected people can spread the disease when they participate in consumption activity with susceptible people. The infection risk will be lower if infected people voluntarily reduce their consumption, but since they will not get infected again, the infection risk is not relevant for their optimization problem. As such, the infected people do not adjust their consumption behavior without an intervention from the social planner.

Susceptible A susceptible person faces the risk of getting infected when she interacts with others in consumption activity. For a person living in H, the interactions can arise from within the region and between the susceptible and infected from the other region, $C_{Ht}^s\left(\hat{I}_t C_{Ht}^i + \hat{I}_t^* C_{Ht}^{i*}\right)$, or when the susceptible agent travels to F, $C_{Ft}^s\left(\hat{I}_t C_{Ft}^i + \hat{I}_t^* C_{Ft}^{i*}\right)$. The following equation describes the risk of getting infected for residents in H

$$\tau_t = \pi_s C_{Ht}^s(\hat{I}_t C_{Ht}^i + \hat{I}_t^* C_{Ht}^{i*}) + \pi_s^* C_{Ft}^s(\hat{I}_t C_{Ft}^i + \hat{I}_t^* C_{Ft}^{i*}) \tag{4}$$

where $\pi_s \in [0,1]$ and $\pi_s^* \in [0,1]$ are the infection parameters in H and F, respectively. These parameters govern the probabilities of getting infected in the respective regions. In the event of a total travel ban between H and F, $C_{Ht}^{i*} = C_{Ht}^{s*} = C_{Ft}^s = C_{Ft}^i = 0$. τ_t then resembles the consumption channel of infection in ERT, and the homogeneous sector scenario in KUX.

It is useful to relate Eq. (4) to the conventional SIR model, in which the infection risk is defined as $\tilde{\tau}_t = \tilde{\pi}_s \hat{\tilde{I}}_t$. In Eq. (4), we introduce dynamics to the infection parameter so that it varies as consumption by infected and susceptible people changes. Assuming that consumption does not change from the steady state and that the disease dynamics are identical across the regions, we can write the infection parameter in the conventional model in terms of the steady steady consumption: $\tilde{\pi}_s = \pi_s C_H^s(C_H^i + C_H^{i*}) + \pi_s^* C_F^s(C_F^i + C_F^{i*})$.

The susceptible person has τ_t probability of getting infected, and $1-\tau_t$ probability of remaining susceptible. As such, the person maximizes the following bellman equation

$$U_t^s = u(C_t^s, N_t^s) + \beta E_t\left[\tau_t U_{t+1}^i + (1-\tau_t)U_{t+1}^s\right]$$

subject to the infection risk Eq. (4) and the budget constraint. The first-order conditions are

$$
\begin{aligned}
C^s_{Ht}: &\quad (1+\rho_t)\lambda^s_{bt} = (1-\upsilon)^{1/\eta}\left(\frac{C^s_{Ht}}{C^s_t}\right)^{-1/\eta}\frac{1}{C^s_t} + \lambda_{\tau t}\pi_s\left(\hat{I}_t C^i_{Ht} + \hat{I}^*_t C^{i*}_{Ht}\right)\\
C^s_{Ft}: &\quad (1+\rho^*_t)(1+\mu^*_t)\lambda^s_{bt} = \upsilon^{1/\eta}\left(\frac{C^s_{Ft}}{C^s_t}\right)^{-1/\eta}\frac{1}{C^s_t} + \lambda_{\tau t}\pi^*_s\left(\hat{I}_t C^i_{Ft} + \hat{I}^*_t C^{i*}_{Ft}\right)\\
N^s_t: &\quad \theta N^s_t = A\lambda^s_{bt}\\
\tau_t: &\quad \lambda_{\tau t} = \beta E_t\left(U^i_{t+1} - U^s_{t+1}\right)
\end{aligned}
$$

where λ^s_{bt} and $\lambda_{\tau t}$ are the respective Lagrange multipliers for the budget constraint and the infection risk.

The above optimality conditions of the susceptible people provide intuitive predictions on their behavior. The relative infection risk between region H and region F determines people's choice of domestic and travel consumption. A higher value of π^*_s, which implies a higher risk of getting infected in region F than in region H, results in the susceptible people voluntarily consuming more domestic goods and less travel-related goods.

Population dynamics In every period, the susceptible people are infected with probability τ_t. Therefore, the newly infected population is given by

$$T_t = \tau_t S_t$$

Accordingly, the law of motion for population dynamics is given by the following set of equations:

$$
\begin{aligned}
S_{t+1} &= S_t - T_t\\
I_{t+1} &= I_t + T_t - (\pi_r + \pi_d)I_t\\
R_{t+1} &= R_t + \pi_r I_t\\
D_{t+1} &= D_t + \pi_d I_t\\
pop_0 &= S_t + I_t + R_t + D_t
\end{aligned}
$$

As with ERT, we assume that the dynamics in the economy begins with a tiny zoonotic infection $I_0 = \varepsilon > 0$. Hence, $S_0 = pop_0 - \varepsilon$. Then, people react to the development of the pandemic and decide on their consumption rationally.

Aggregate variables The economy's aggregate consumption and labor are summed from all live agents

$$
\begin{aligned}
C_t &= S_t C^s_t + I_t C^i_t + R_t C^r_t\\
N_t &= S_t N^s_t + I_t N^i_t + R_t N^r_t
\end{aligned}
$$

Government's budget constraint is

$$\begin{aligned}&\left(S_t + I_t + R_t\right) A\Gamma_t \\ &\qquad = \rho_t \left(S_t C^s_{Ht} + I_t C^i_{Ht} + R_t C^r_{Ht}\right) + \left(\rho_t + \mu_t + \rho_t \mu_t\right) \left(S^*_t C^{s*}_{Ht} + I^*_t C^{i*}_{Ht} + R^*_t C^{r*}_{Ht}\right)\end{aligned}$$

The preceding descriptions provide details on the behavior of the three types of people in region H in the model. The policy instruments on domestic consumption and travel are exogenous to the agents. In what follows, we describe the social planners' problems and the corresponding solutions for the policy instrument variables.

2.3 Social planners' problems

There is one social planner residing in each region. Each social planner calculates the societal welfare in her region from the lifetime utility of all residents. In the case of H, the social welfare is defined as the lifetime utility of all residents in H starting from period 0:

$$\mathcal{W}_0 = S_0 U^s_0 + I_0 U^i_0 \tag{5}$$

where

$$U^s_0 = u^s_0 + \beta \left[\left(1 - \tau_0\right) U^s_1 + \tau_0 U^i_1\right] \tag{6}$$

$$U^i_0 = u^i_0 + \beta \left[\left(1 - \pi_r - \pi_d\right) U^i_1 + \pi_r U^r_1\right] \tag{7}$$

as defined in the model. In the case of F, the social welfare is given as

$$\mathcal{W}^*_0 = S^*_0 U^{s*}_0 + I^*_0 U^{i*}_0 \tag{8}$$

where U^{s*}_0 and U^{i*}_0 are defined analogously.

No policy Social planners adopting the *lazzie-faire* approach may choose not to impose any policy restriction on consumption or travel. This scenario is characterized by all policy instruments not being used, in other words,

$$\mu_t = \mu^*_t = \rho_t = \rho^*_t = 0.$$

Cooperation Upon cooperation, the two social planners jointly maximize the social welfare of all residents in both regions. In this case, the objective function of the collaborating social planners is

$$\max \mathcal{W}_0 + \mathcal{W}^*_0.$$

The set of constraints consists of all equations at the competitive equilibrium. We then obtain the first order conditions with respect to all endogenous variables and the four policy instru-

ments. For the 48 equations solving the competitive equilibrium listed in Appendix B, the system giving the Ramsey solutions contains $2 \times 48 + 4 = 100$ equations.

Non-cooperation Alternatively, in the non-cooperative regime, the social planner in region H maximizes the social welfare $\mathcal{W}_0$ in her own region while taking the entire paths of foreign policy tools, consumption tax ρ_t^* and travel restrictions μ_t^*, as given. Simultaneously, the social planner in region F maximizes the social welfare $\mathcal{W}_0^*$ in her region while taking the entire path of the home policy tools, consumption tax ρ_t and travel restrictions μ_t, as given. This is known as an open-loop Nash game.

The set of constraints is the same as in the cooperative equilibrium. Each social planner derives first-order conditions with respect to all endogenous variables and her two policy instruments, taking policies in her counterpart as given. For the set of 48 equations at the competitive equilibrium, the system giving the Ramsey solutions at the open-loop Nash equilibrium consists of $3 \times 48 + 4 = 148$ equations.

In addition to the two optimal policy regimes, scenarios including border closure, border control, as well as no policy intervention are considered. They are introduced later in the paper.

Welfare loss We calculate the consumption-equivalent measure of welfare loss as

$$\mathcal{L}_0 = \left[\exp\left[(1-\beta)\left(\mathcal{W}_0^{alt} - \mathcal{W}_0^{baseline}\right)\right] - 1\right] \times 100\%$$

which tells the percentage of consumption that one needs to be compensated in order to change from the baseline to an alternative regime.

2.4 Computation strategy

The model is solved in Dynare 4.6.4. All agents are aware of the pandemic and all policy interventions in a reasonably long time frame. We note that assuming an infinite time horizon does not provide plausible interpretation because it implies that the pandemic stays forever with no cure in the foreseeable future. We also note that assuming too long a time horizon, albeit finite, does not provide sensible results either because it diminishes the effects of policy actions and the negative externality of no policy. This assumption provides us with a basis to perform perfect foresight simulations.

We assume that people are able to plan around six years since the beginning of the pandemic, which translates into 300 weeks since the initial infection. Given that people are already being vaccinated as of June 2021, we believe that the assumption is consistent with policy planning horizon. It is also consistent with existing literature.

A set of guessed values are given to the model as the initial solution. Dynare then adjusts the series until the solutions are found. After the computation, the social welfare of the social

planner H and F is calculated according to Eq. (5) and Eq. (8), respectively

$$\hat{\mathcal{W}}_0 = \hat{\tilde{S}}_0 \hat{\tilde{U}}_0^s + \hat{\tilde{I}}_0 \hat{\tilde{U}}_0^i \tag{9}$$

$$\hat{\mathcal{W}}_0^* = \hat{\tilde{S}}_0^* \hat{\tilde{U}}_0^{s*} + \hat{\tilde{I}}_0^* \hat{\tilde{U}}_0^{i*} \tag{10}$$

while the welfare under cooperation is calculated according to

$$\hat{\mathcal{W}}_0 + \hat{\mathcal{W}}_0^* \tag{11}$$

where the hats-tildes denote simulated values.

2.5 Parameters

Our baseline simulations assume two symmetric regions. All parameters are identical across the regions. Following ERT, we set the productivity parameter A to be 39.835, and the labor elasticity parameter θ to be 0.001275. Both parameters give weekly consumption of US$1,115.6 and 28 hours of work. They also correspond to a value of statistical life of US$9m, following the calculation in Krueger et al. (2020). The discount factor is $\beta = 0.96^{1/52}$. The share of travel-related consumption in the consumption basket υ is set to be 5 percent. We set $\eta = 3$ to imply a relatively low elasticity of substitution between domestic and travel-related goods. It takes 18 days for an infected person to recover or die. Given a case fatality rate of 0.5%, the weekly probability of death is $\pi_d = 7 \times 0.005/18$. The removal rate is $\pi_r + \pi_d = 1/18$. We use $\pi_s = 4.05 \times 10^{-7}$ as the probability of infection as it leads to a decline in aggregate consumption of 10% at the peak of the economic recession. The pandemic begins with 0.1% infected population and 99.9% susceptible population in each region in period 0.

3 Baseline simulations

In the baseline simulations, regions are hit by an initial infection of the same size. All responses are therefore identical and we only show the dynamics in H.

3.1 Cooperative equilibrium

The juxtaposition of the solutions for the cooperative equilibrium and the competitive equilibrium (no policy) are shown in Fig. 1. The green lines show the dynamics in the economy when two regions collaborate to achieve the maximum welfare for residents in both regions. The black dotted lines assume no policy is implemented to contain the pandemic. The horizontal axes show the number of weeks after the initial infection.

The cooperative equilibrium shows an exclusive emphasis on domestic containment and negligible travel restrictions. At the onset of the outbreak, domestic containment measures are immediately implemented. In our model, the domestic containment measures are in the form of a consumption tax, which reduces consumption, and hence interactions between the

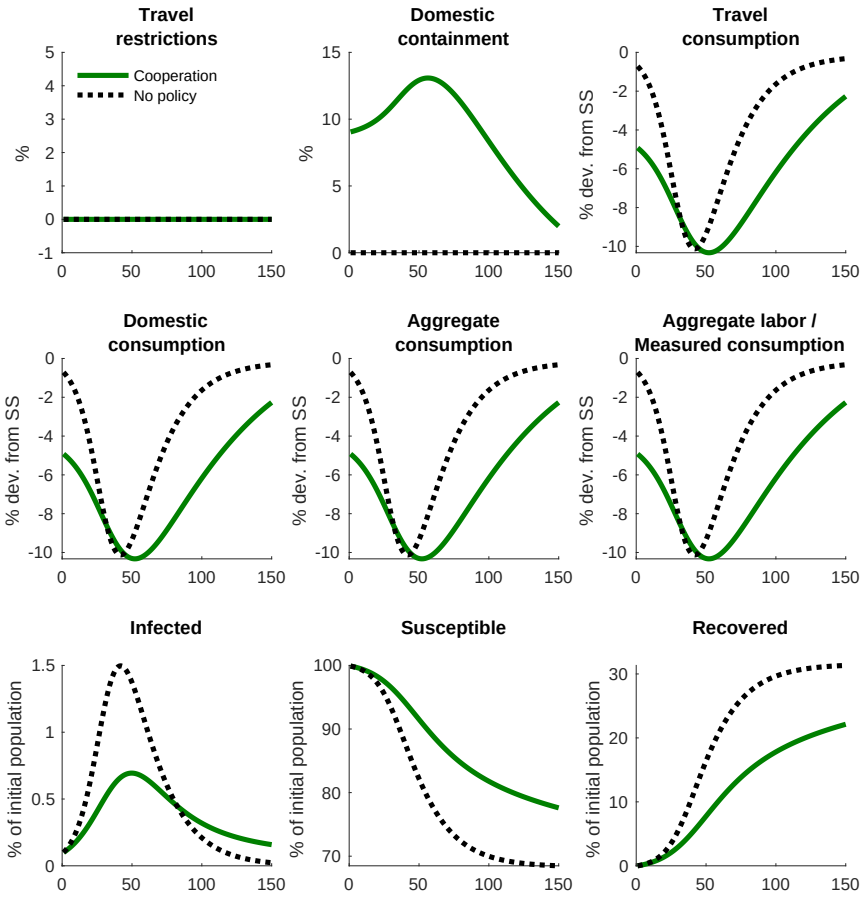

Figure 1: Cooperative equilibrium.

infected and susceptible people. For the parameters in our simulations, the consumption tax is about 13% at the peak of the pandemic. Aggregate consumption and its components are generally lower compared to the no-policy scenario. As a result of the lower consumption (level of interactions), the infection curve is flatter, and there is a high stock of susceptible population in the long run.

Travel restrictions, however, do not appear to be necessary in the cooperative equilibrium. This is partly because the baseline simulations assume symmetry across the two regions. As the two regions are identical in the development of the pandemic and the disease parameters are also identical, implementing travel restrictions does not make either region better off. In our subsequent results, travel restrictions play a role when two regions are at different stages of the pandemic.

3.2 Non-cooperative equilibrium

In Fig. 2, we compare the non-cooperative equilibrium (green dash line) with the cooperative equilibrium in Fig. 1 (green solid line).

The non-cooperative equilibrium features high travel restrictions. Similar to domestic containment measures, the travel restrictions are imposed in the form of higher costs of cross-border

Table 1: Consumption-equivalent welfare loss from cooperative equilibrium.

	Non-cooperation	Border control ($\mu_t = \mu_t^* \to \infty$)	Border closure ($C_{Ft} = C_{Ht}^* = 0$)	No policy
Symmetric ($I_0^* = I_0 = \varepsilon$)	-0.109	-0.446	-0.456	-0.162
Asymmetric ($I_0^* > I_0 = 0$)	-0.106	-0.472	-0.024	-0.152
Region H	-0.100	-0.503	0.399	-0.155
Region F	-0.112	-0.441	-0.445	-0.150

Note: Consumption-equivalent welfare losses are percentages of consumption goods that an agent needs to be compensated in order to move to an alternative scenario. A negative number indicates a lower welfare level compared to that in the cooperative equilibrium, vice versa. Non-cooperation refers to the open-loop Nash equilibrium. A border control occurs when regions impose high travel restrictions but still allow cross-border travel. A border closure is equivalent to a travel ban. In the no-policy scenario, no domestic containment or travel restriction is imposed. The symmetric case refers to when regions H and F are identical in terms of economic fundamentals, disease characteristics, and the development stage of the pandemic. The asymmetric case is one when the pandemic originates from region F.

travel. For the parameters we use, the travel costs are about 50% higher than that under cooperation. The immediate effect of the travel restrictions is a drastic decline in travel consumption by nearly 70%. Domestic consumption, however, fall less due to the substitution effect between the components in the consumption basket. Domestic containment is less strict.

The lower cross-border travel, however, merely results in a slightly lower infection curve compared to the cooperative equilibrium. Agents end up with lower aggregate consumption. As an assessment of the welfare effect, we present in Table 1 the consumption-equivalent welfare losses of various scenarios from the cooperative equilibrium. Negative numbers imply that agents need to be compensated a percentage of their consumption in order to reach the same level of welfare as in the cooperative equilibrium. In other words, agents are worse off. From the table, we see that the non-cooperative equilibrium leads to a lower welfare level as compared to the cooperative equilibrium. Nonetheless, agents are still better off than in a no-policy scenario.

3.3 Border closure and control

In fighting against the pandemic, border closure has become a commonly adopted policy tool. This entails a complete ban on cross-border travel between the regions. In some scenarios, which we call them border controls, social planners may allow minimal travel for essential purposes. The difference between a border closure and a border control is that the former enforces that $C_{Ft} = C_{Ht}^* = 0$, and the latter sets travel restrictions at extremely high levels, i.e $\mu_t = \mu_t^* \to \infty$.

The formulation for these two border management tools are similar to the non-cooperative solutions. The difference is in that the social planners give up on optimizing travel restrictions in border management. They set travel restrictions close to or at the limit and rely on domestic containment to attain the highest welfare.

We show the dynamics under border closure in Fig. 3 (green dotted line). The obvious change from the cooperative equilibrium is the 100% reduction in travel consumption. This leads to higher domestic consumption due to the substitution effect. Aggregate consumption

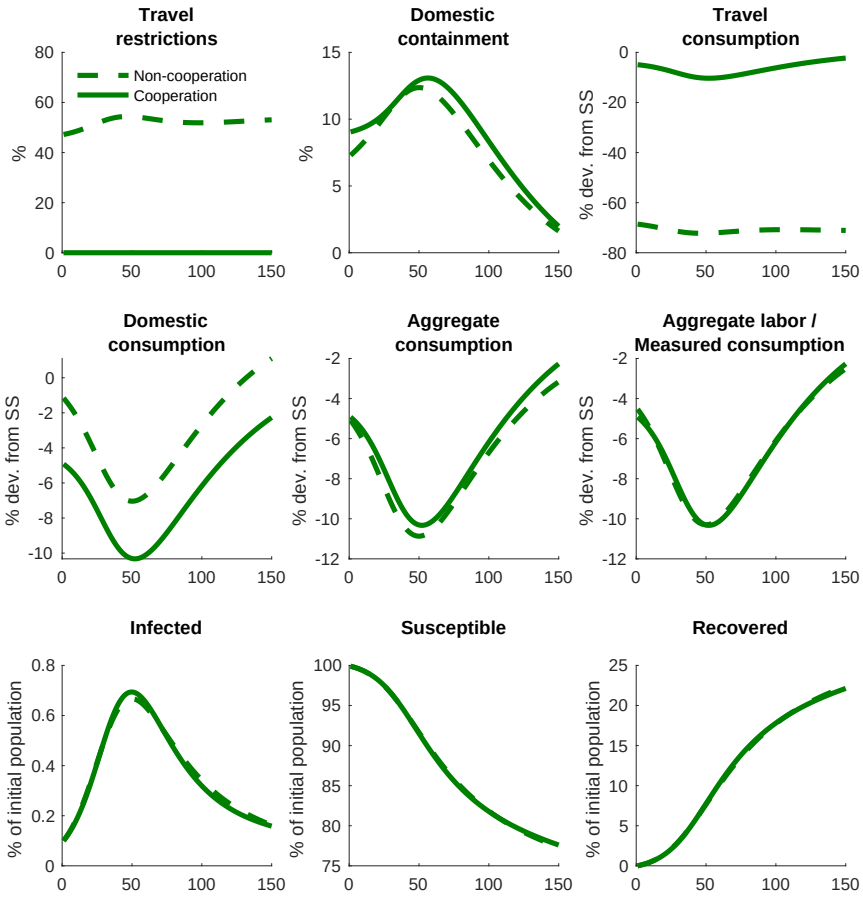

Figure 2: Non-cooperative equilibrium.

is lower, as domestic consumption is not a perfect substitute of travel consumption. There is a larger welfare loss compared to the no-policy scenario, as calculated in Table 1. We note that when the two regions are symmetric, a border closure and a border control result in visually the same dynamics. The welfare outcomes are also similar.

It is worth highlighting that the welfare losses from border closure and border control are the highest among all the scenarios we analyze. This is explained by the reduction in consumption which is not compensated by any improvement in the health status of the population, due to the symmetric infection development. In other words, a dead-weight loss is created due to the border closure/control.

4 Asymmetric pandemic development

Our baseline simulations assume that regions are identical. An alternative but equally important assumption is that two regions are at different stages of a pandemic. We illustrate this scenario by simulating a pandemic which originates from only one of the two regions, and analyzing how policies are implemented under cooperative and non-cooperative equilibria. Without loss of generality, we assume that the initial infection occurs in F but not in H. Except in the case of a border closure, a pandemic originating from region F eventually spreads across the border.

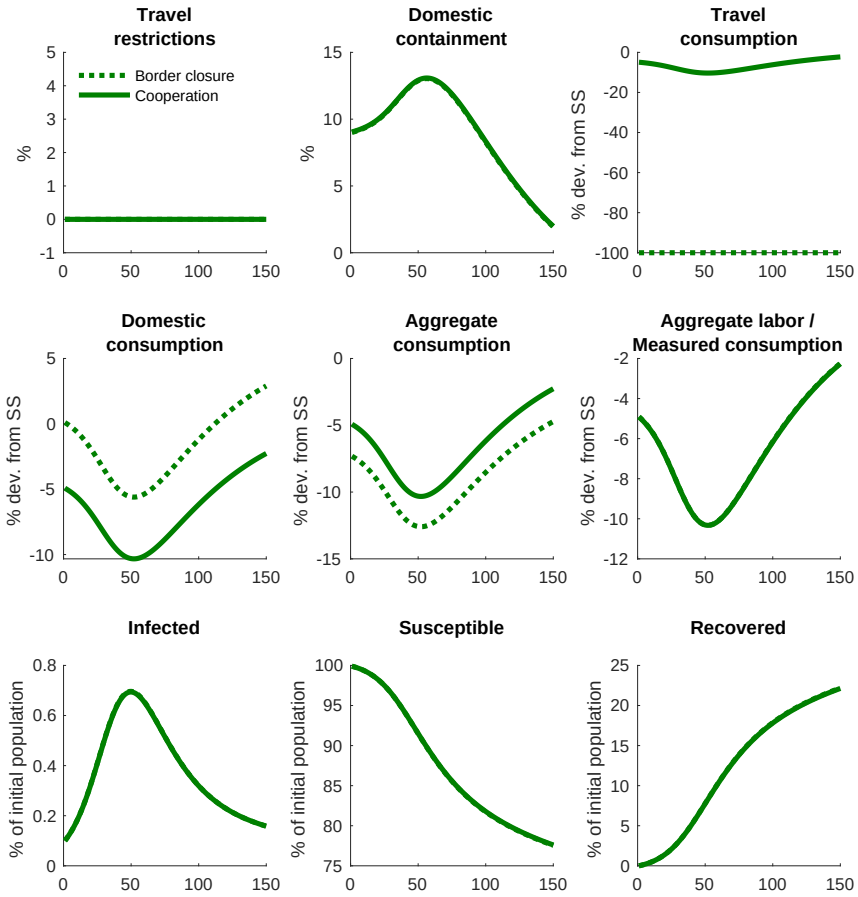

Figure 3: Border closure.

4.1 Cooperative equilibrium

As with the baseline simulations, we begin with the cooperative equilibrium in which social planners in both regions collaborate to maximize the welfare of all residents. The economic and population dynamics under the cooperative equilibrium are shown in Fig. 4.

In general, when regions cooperate, policies tend to eliminate the differences in both population and economic dynamics, despite the regions' initial health status. This means that the differences in the policies are largely associated with those in their infection curves. As the pandemic spreads across the border, the infection curves converge. We see that the policies and economic dynamics converge to the cooperative equilibrium under the symmetric setting shown in Fig. 1. Compared to a no-policy scenario, the cooperative equilibrium delivers a better welfare (see Table 1).

An interesting outcome is that at the onset of the pandemic, the social planners in H and F impose opposite travel restrictions on travelers from the other region. In particular, there are negative travel restrictions in F, also interpreted as subsidies, for travelers from H, but high travel restrictions in H for travelers from F. It is easy to understand that the high travel restrictions imposed on travelers from F are needed to slow down the cross-border spread of the pandemic. As for the subsidies provided to travelers from H, one needs to relate

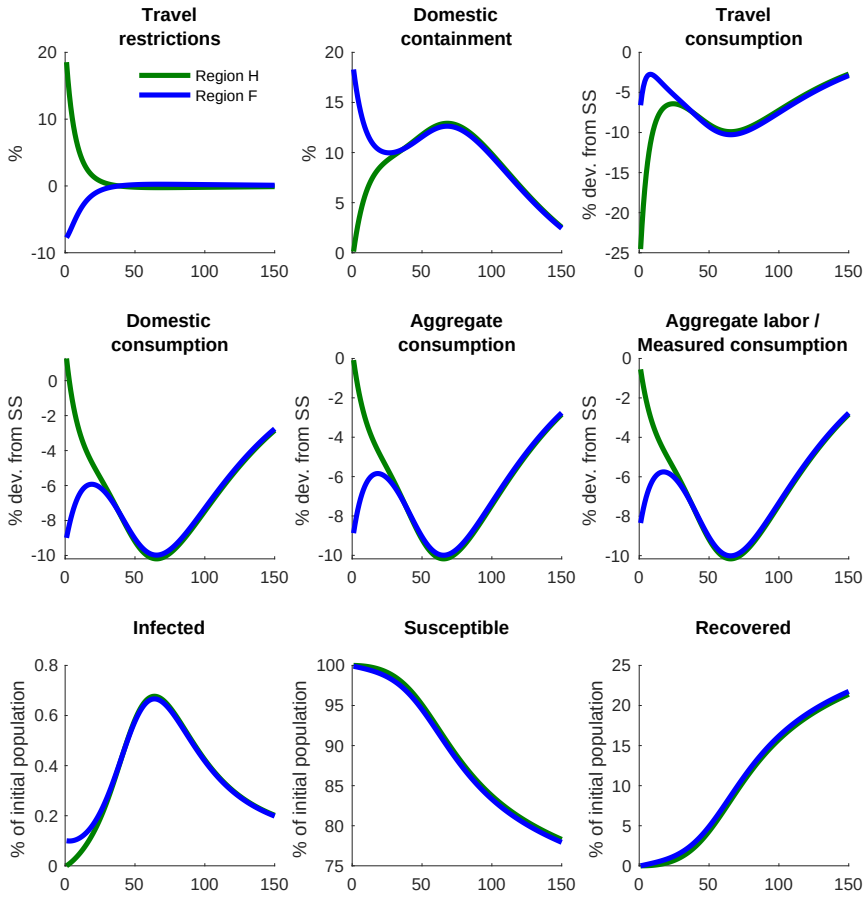

Figure 4: Initial infection in F. Cooperative equilibrium.

it to the consumer behavior at the beginning of the pandemic. As the pandemic originates from F, consumers in H tend to voluntarily reduce their travel consumption, substituting it with domestic consumption. This benefit of lower health risk due to agents' voluntary choice, however, does not outweigh the cost of lower aggregate consumption. As a result, subsidies are needed to correct the excessive decline in travel consumption by agents in H. Subsequently, as the pandemic spreads across the border, as seen from the overlapping population dynamics, the travel restrictions in both regions converge.

A similar pattern is observed for the domestic containment. Region H imposed almost zero domestic containment when the pandemic arises in F. Whereas, in region F, strict containment measures are imposed to limit the consumption activity in the region. As the pandemic spreads across the border, domestic containment in H needs to be tightened. The opposing domestic containment measures in the two regions eventually drive the infection in both regions to the same level.

4.2 Non-cooperative equilibrium

In the non-cooperative equilibrium, social planners maximize the welfare of their respective regions. Fig. 5 presents the dynamics under the non-cooperative equilibrium.

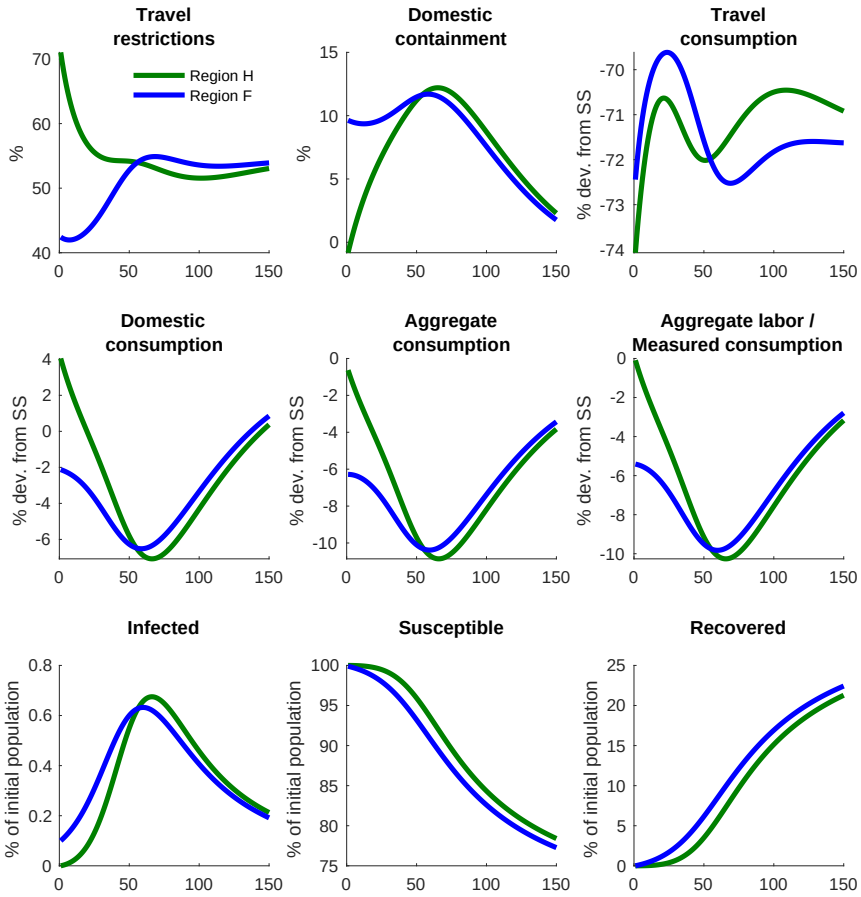

Figure 5: Initial infection in F. Non-cooperative equilibrium.

Similar to the results for the cooperative equilibrium, travel restrictions and domestic containment tend to bring the two infection curves closer, as well as the economic dynamics. This again shows that policy responses at the noncooperative equilibrium are associated with the development in the infection curves, which eventually converge as the pandemic travels across the regions.

The starkest departure from the cooperative equilibrium is the substantially high travel restrictions in both regions. Both regions impose travel restrictions which increase the travel cost by 40-70%. From the perspectives of the social planner in region H, travelers from F need to be deterred to the extent that the cost of heightened health risk due to the travelers do not exceed the receipts from the travelers. Whereas, as a social planner in F, travelers in H also need to be deterred, but due to the lower initial infection in H, the health risk is lower. These high travel restrictions result in drastic decline in travel consumption. In both regions, agents reduce their travel consumption by more than 70%.

4.3 Border closure and control

The most surprising but intuitive results are with the border closure and border control. We have explained that a border control differs from a border closure in that minimal essential travel

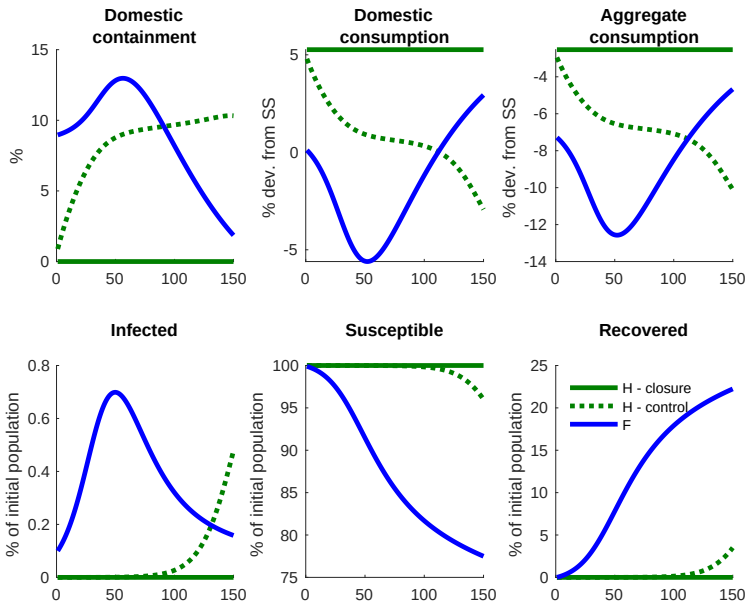

Figure 6: Initial infection in F. Non-cooperative equilibrium with border closure and border control.

is allowed. To region H, which is not the origin of the pandemic, a border closure completely blocks the spread of the disease. A border control, on the other hand, allows an arbitrarily small amount of infected people to travel across the borders. The implication is that it is just a matter of time that this small amount of infected people eventually translates into substantial infection in the region.

We show the population and economic dynamics in Fig. 6. As expected, under a border closure, variables in H are not affected at all. As for border control, the social planner in H imposes strict domestic containment from the beginning of the pandemic, preventing travelers from F from taking part in domestic consumption activity. This domestic containment leads to the first "wave" of decline in aggregate consumption. The infected population eventually reaches the critical mass after 100 weeks, when agents in the economy understand the health risk and voluntarily avoid consumption. This behavior translates into a second "wave" of consumption decline.

4.4 Welfare implications

Table 1 summarizes the welfare losses should regions decide not to cooperate. Under the assumption of asymmetric pandemic development, we calculate the welfare losses for respective regions and the overall for both regions. This helps to us to identify any Pareto improvement should regions decide to cooperate. On average, none of the policies provides better welfare than that from cooperation between the regions.

Border closure delivers the best average welfare outcome should regions decide not to cooperate. This is so because region H is at its pre-pandemic state as region F is undergoing the pandemic. Should regions decide to cooperate, region H suffers lower welfare while region

F benefits from a higher welfare. It is therefore not Pareto optimal if the policy framework transits from border closure to cooperation.

Border control gives the worst average welfare outcome. Due to the prolonged period of infection in H, border control ends up the least favorable solution for H. Opening up the border and cooperating, in the case of a border control, are found to be Pareto optimal, as both regions benefit from higher welfare.

The welfare outcome from a non-cooperation Nash game is between those of border closure and border control. This is because it allows social planners to set the travel restrictions according to the planning objectives. It is expected to give better welfare outcome than a border control. Should regions transit from non-cooperation to cooperation, the travel restrictions are eliminated, and people derive utility from cross-border travel. Both regions benefit from higher welfare. There is a Pareto improvement.

5 Vaccination and pre-departure tests

In this section, we alter some assumptions in the baseline model to make it closer to reality. For instance, vaccines are now being introduced to the general public, reducing the health costs of the pandemic. Also, infected people are usually prohibited from traveling as they can be easily identified by pre-departure tests. We introduce the scenarios of vaccination and pre-departure tests in the subsequent subsections to see their welfare effects.

5.1 Vaccination

Our earlier simulations find that welfare losses are large when social planners implement border controls instead of border closures. This is due to the fact that, unlike a complete cut-off in cross-border infection in a border closure, any arbitrarily small amount of infection across the border eventually results in a large-scale infection that spans a longer time period. Despite this theoretical finding, border control remains a popular tool amid the pandemic. Here we show that one remedy for the delayed infection due to border control is the timely arrival of the vaccine.

We recognize that a vaccine helps to prevent critical illness, but may or may not reduce the infection rate of the pandemic. In our model, we assume that the probability of death, π_d, decreases in the region where the residents are vaccinated. The reduction in the probability of death reduces the health costs of the pandemic, trading off the future costs as small amount cross-border infections accumulate. As such, if the death probability can be eliminated in a timely manner, the future health costs will be small.

We simulate vaccination plans spanning between 0 and 5 years. In the ideal case, the population is vaccinated at the onset of the pandemic, and the value of π_d is set to 0 throughout the simulated periods. For any vaccination plan set to be completed with n years, the value of π_d decreases linearly to 0 between period 0 and the end of the nth year. We aim to find out how a social planner adopting a border control should design their vaccination plan to contain the

future health costs. As in our previous sections, our discussion focuses on both the dynamics of the variables and the welfare implications.

We simulate a linear decline in π_d in H as vaccines roll out. Residents in F are assumed not to be vaccinated. Both social planners implement border controls and the domestic containment is at the Nash equilibrium. Welfare losses are shown in Fig. 7. The horizontal axis represent the number of years after the onset of the pandemic when H gets every resident vaccinated. In Fig. 8, we show the dynamics when everyone in H is vaccinated in 2 year and in 4 years against a scenario with no vaccine available. We provide three observations based on these figures.

First, vaccinating the population within two years offers the same level of welfare gain between border control and border closure. We see from Fig. 7 that welfare in H remains on par with that in the case of a border closure, if everyone in H is vaccinated within two years. Should the vaccination plan takes longer than two years to complete, the welfare gain to H would be lower. As will be elaborated soon, this is because the health costs pick up ahead of the vaccination rate. We note that a vaccination plan of five years nearly wipes out all the welfare gain that would have been achieved with border control.

Second, a large spike in the infection curve is likely, due to the reduced probability of death. We see in Fig. 8 that with a two-year vaccination plan, there is a large spike in the infection curve in the third year. The peak infection is much larger than the no-policy scenario found in Fig. 1. This is because as the death probability is substantially lower, people may not be too concerned about being infected. In reality, we do observe some policy makers cautiously proceed with resuming economic activity despite that infected cases are still on the rise. The most notable examples are the European countries where vaccination passports are being discussed. A key factor that gives them the confidence is the high vaccination rates in the population. Naturally, as people return to economic activity, human interactions increase, hence the high infection.

Third, domestic containment is gradually lifted towards the end of the vaccination plan. As the health costs are lower with the vaccinated population, it is justifiable that domestic containment can be lifted. Domestic economic activity cannot be suppressed indefinitely. Once the health costs are outweighed by the economic costs, domestic containment has to be lifted to revive economic activity. Contrary to the no-vaccine case, consumption does not experience a second wave of decline.

Taken together, our simulation results reveal that border control can be used as an interim measure as the region vaccinates its people. It is important that social planners design the vaccination plan appropriately and in a timely manner, so as to maintain the benefits of a border control. One should also expect spikes in the infection curve as the population is vaccinated and economic activity resumes, but these spikes should not be a cause of alarm if vaccination proceeds as planned.

5.2 Pre-departure tests

Our baseline simulations did not consider pre-departure tests, which are now mandatory before people embark on cross-border travel. As mentioned in the beginning of the paper, social

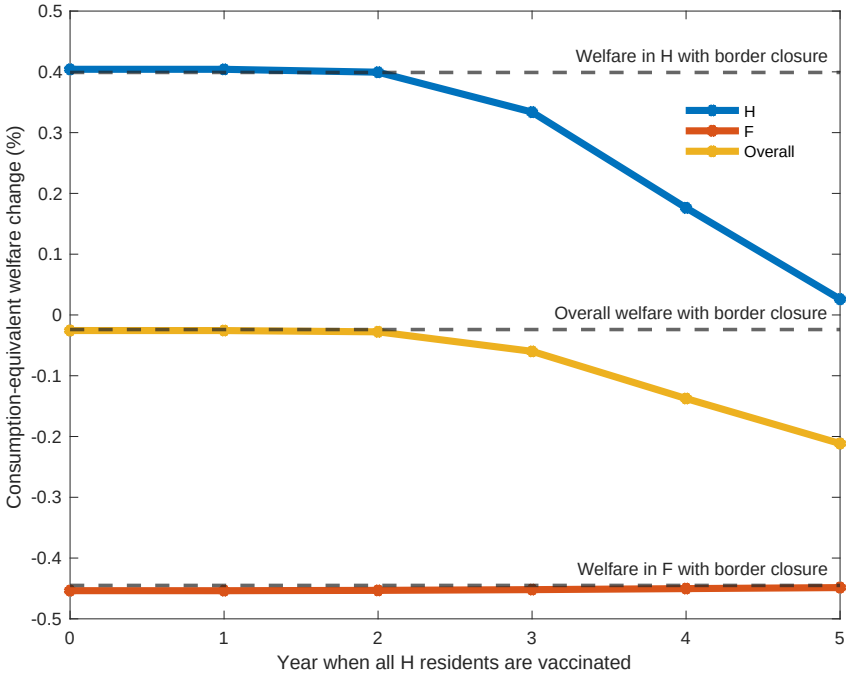

Figure 7: Welfare losses and vaccination plan in H.

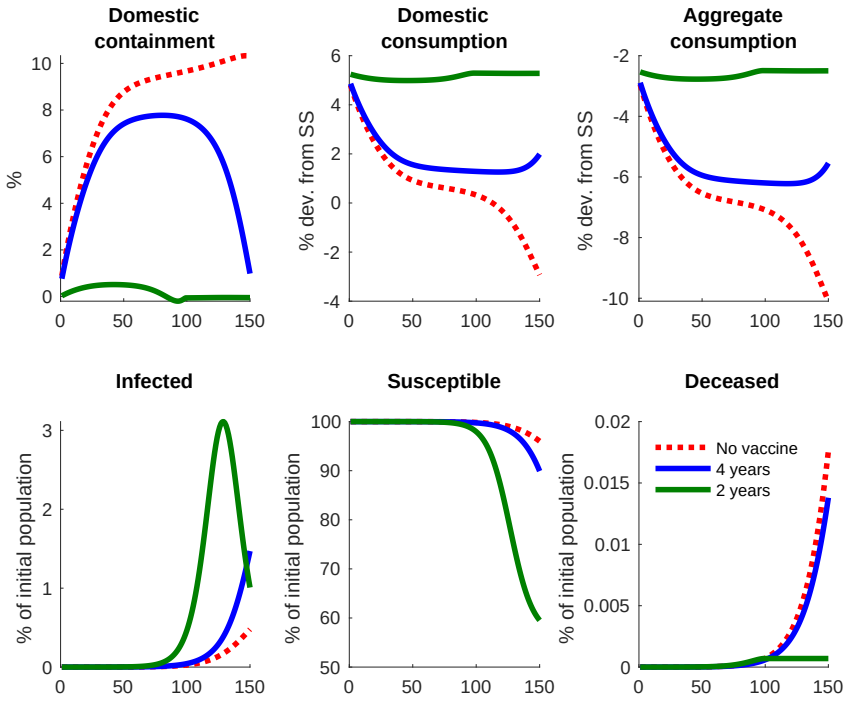

Figure 8: Non-cooperative equilibrium with border control. Initial infection in F. Vaccination plan in H.

planners are wary of imported infection. Pre-departure tests are helpful in identifying the infected people and preventing the pandemic from spreading across the border. We simulate a situation when it is possible to prohibit infected agents from traveling. Mathematically, it means that social planners are able to ensure that

$$C^i_{Ft} = C^{i*}_{Ht} = 0$$

It follows that the infection risks due to traveling infected people vanish and the overall infection risk is

$$\tau_t = \pi_s C^s_{H,t} I_t C^i_{H,t} + \pi^*_s C^s_{F,t} I^*_t C^{i*}_{F,t}$$

Because infected agents are not able to travel, the above infection risk is lower than the one in the baseline setup.

We find that pre-departure tests are useful in bringing travel consumption back to normal at the cooperative equilibrium but not at the non-cooperative equilibrium. As seen in Fig. 9, with some travel subsidies introduced, travel consumption is almost back at the pre-pandemic level. Some domestic consumption is substituted with travel consumption. The change in welfare is calculated to be 0.0035% of consumption, which is a slight improvement from the cooperative equilibrium without pre-departure tests.

Dynamics at the non-cooperative equilibrium are shown in Fig. 10. Similarly, travel restrictions are relaxed, leading to small recovery in travel consumption. Domestic containment is stricter, as infected people consume and interact more domestically. Domestic consumption is lower. Health costs are lower as seen from the flatter infection curve. The overall welfare effect is an improvement equivalent to $3.2 \times 10^{-5}\%$ of consumption, which is negligible.

In summary, our results show that although pre-departure tests are nowadays commonplace, their implementation is justifiable only when social planners agree to cooperate. The net benefits of pre-departure tests are minimum if regions decide not to cooperate.

6 Travel bubbles

In this section, we analyze two examples of cooperative travel arrangements. Regions taking parts in cooperative travel arrangements are usually not homogeneous as in our baseline simulations. They could differ in economic environment, travel demand and the development of the pandemic. The most cited examples of cooperative travel arrangements in Asia and Oceania are perhaps between Singapore and Hong Kong, and between Australia and New Zealand, which are commonly known as "travel bubbles". The "travel bubbles" aim to facilitate easier bilateral travel for all purposes. Prior to these initiatives, Singapore, Hong Kong, Australia, and New Zealand all imposed stringent travel restrictions, deterring foreigners from entering their territories. With the "travel bubbles" in sight, we use our model to assess the welfare effects if these regions shift from the earlier non-cooperative arrangements to the ongoing or

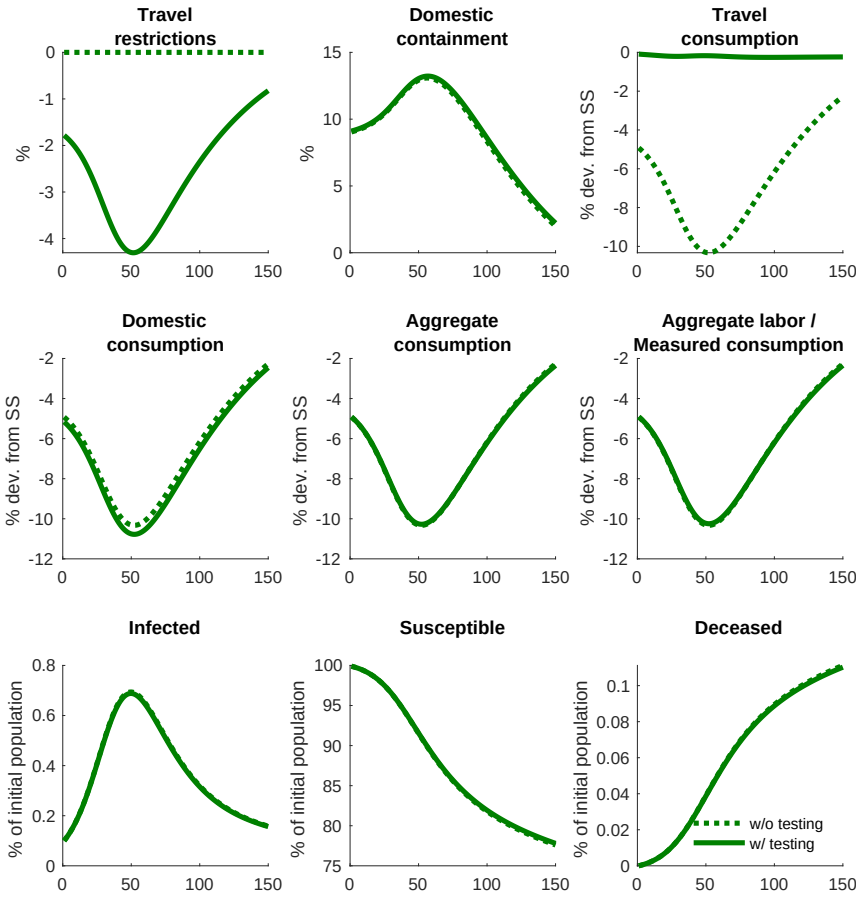

Figure 9: Cooperative equilibrium with pre-departure testing.

forthcoming "travel bubbles". In what follows, we calibrate the model according to these two cases, and derive the corresponding welfare outcome, measured in dollar terms. While calibrating the model, we use population to proxy the GDP of the region, assuming all regions in stake are similar in per capita income.

6.1 Singapore – Hong Kong

The travel bubble between Singapore and Hong Kong was announced twice in November 2020 and April 2021, but was both postponed before the official launch due to spikes of new infections. On November 11, 2020, Singapore and Hong Kong agreed to launch a travel bubble officially starting from November 22, 2020, but it was deferred until early December and then beyond 2020 due to the sudden spike of new infections in Hong Kong (CNN, 2020; BBC, 2020). On April 26, 2021, both regions confirmed the official re-launch of travel bubble on May 26, 2021, but it was once again put on hold on May 17, 2021 due to the heightened measures in Singapore (ChannelNewsAsia, 2021a,b). In the press statement on June 10, 2021, Singapore and Hong Kong announced that the date of launching of travel bubble would be reviewed again in early July (HKSAR, 2021).

The case of travel arrangements between Singapore and Hong Kong is close to our baseline

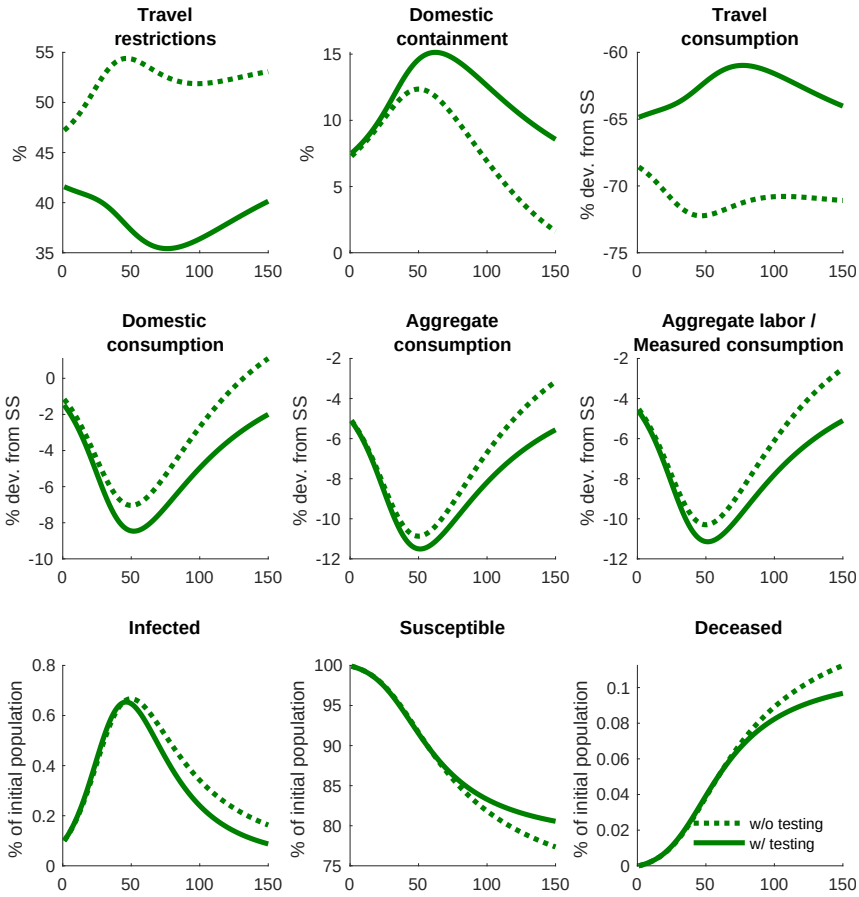

Figure 10: Non-cooperative equilibrium with pre-departure testing.

model. The two regions are similar in terms of GDP. The differentiating factor from the baseline model is in the uneven demand for bilateral travel by respective residents. Due to the close proximity and economic ties with mainland China, it is not surprising that Hong Kong residents have disproportionately higher preference for traveling to and from the mainland than anywhere else in the world. Whereas, as an independent nation, Singapore residents' travel preferences may be more diversified. Hence, it is expected that, on average, Singapore residents demand more travel to Hong Kong than Hong Kong residents' demand for travel to Singapore. The unequal demand for bilateral travel may lead to uneven welfare outcome for the two regions.

Table 2 summarizes the key economic indicators. As GDP is similar between Singapore and Hong Kong, we assume that the two regions are of the same size. We fix all other parameters as the baseline model, and only change the share of bilateral travel spending accordingly. We use 0.307 percent and 0.169 percent as the share of bilateral travel spending for Singapore and Hong Kong, respectively. Calculating for 300 periods, we obtain the simulated paths for the optimal policies shown in Fig. 11.

The simulated paths are similar to those in our baseline simulations. Figure 11 shows that the travel bubble arrangement between Singapore and Hong Kong promotes almost zero cross-border travel restrictions. Domestic containment and infection curves in both regions are also similar under the cooperative equilibrium and non-cooperative equilibrium. This shows that

Table 2: Parameters of Singapore and Hong Kong.

	Singapore	Hong Kong
Private Consumption Expenditure (USD bn)	133.48	251.87
Travel spending in HK (USD mn)	409.77	
Travel spending in SG (USD mn)		426.26
Share of bilateral travel spending in consumption	0.307%	0.169%
Value of travel bubble (USD per capita)	1,346.50	-76.40
Overall value of travel bubble (USD per capita)	635.10	

Sources: CEIC Database, Xinhuanet

there is not much change in infection cases when the travel bubble is established. Overall there is a welfare gain from cooperation with higher travel consumption and overall consumption. The welfare implications for the individual regions, however, are different.

We translate the welfare losses defined earlier into dollar values using the value of statistical life. Following KUX, we calculate the value of statistical life as

$$\text{VSL} = \frac{\beta}{1-\beta}\left(\log C - \frac{1}{2}\right),$$

and the value of travel bubble as

$$\frac{1}{100} \cdot \text{VSL} \cdot \mathcal{L}_0 \cdot C$$

Overall, the value of Singapore-Hong Kong travel bubble is 635.1 USD per capita. Individually, the travel bubble arrangement delivers higher welfare to Singapore than to Hong Kong. Singapore experiences a gain of 1,346.5 USD per capita under travel bubble, while Hong Kong experiences a small loss of 76.4 USD per capita. This is because Singapore residents demand more travel-related consumption in Hong Kong than the other way round. The small welfare loss in Hong Kong would vanish with a slightly higher share of travel consumption by Hong Kong residents at 0.181 percent, holding other factors unchanged. This potentially opens up room for negotiation for small compensations to Hong Kong residents to make the travel bubble mutually beneficial.

6.2 Australia – New Zealand

On December 14, 2020 Australia and New Zealand first discussed establishing a quarantine-free travel bubble during the first quarter of 2021 (NZ Herald, 2020). The quarantine-free travel bubble was officially announced on April 6, 2021, and then launched on April 18, 2021 (Australian Government Department of Home Affairs, 2021).

The case of travel arrangements between Australia and New Zealand is more distinguishable from our baseline model. New Zealand has closer ties with Australia. On average, New Zealand residents travel more to Australia than Australian residents do to New Zealand. The two regions are also different in terms of their economic sizes. The size of Australian GDP is around 7 times of that of New Zealand. The difference in GDP may be a factor in addition to unequal travel

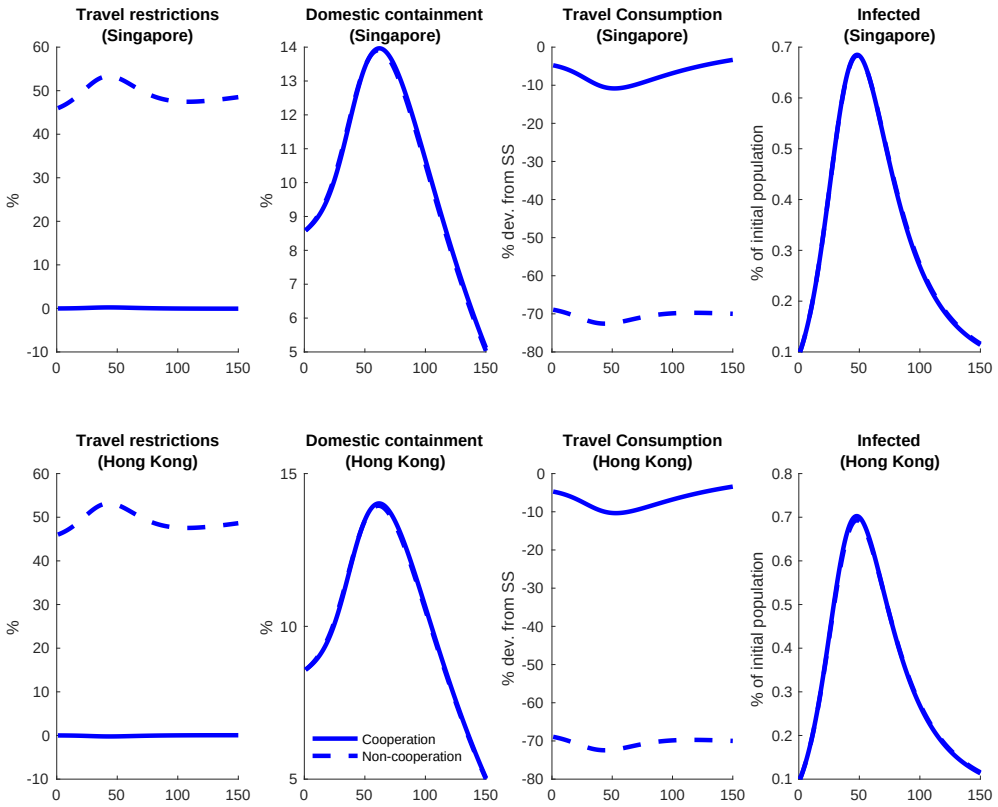

Figure 11: Cooperative and non-cooperative equilibrium for Singapore and Hong Kong.

openness that causes uneven welfare outcome.

The key economic indicators are summarized in Table 3. In the model, we fix all other parameters as in the baseline model, and change the share of bilateral travel spending and GDP accordingly. We use 0.258 percent and 1.620 percent as the respective share of bilateral travel spending for Australia and New Zealand. The GDP size of Australia is calibrated as 7 times of New Zealand's. Calculating for 300 periods, we obtain the results in Fig. 12.

The cooperative travel arrangement between Australia and New Zealand does not promote free travel as in the Singapore – Hong Kong case. There is still a sizable travel restriction in Australia under the cooperative equilibrium. From figure 12, we can see that travel restriction

Table 3: Parameters of Australia and New Zealand.

	Australia	New Zealand
Private Consumption Expenditure (USD bn)	760.98	121.27
Travel spending in NZ (USD mn)	1,961.00	
Travel spending in AU (USD mn)		1,965.00
Share of bilateral travel spending in consumption	0.258%	1.620%
Value of travel bubble (USD per capita)	-412.30	5,347.40
Overall value of travel bubble (USD per capita)	307.80	

Sources: CEIC Database, Budget Direct, Tourism New Zealand

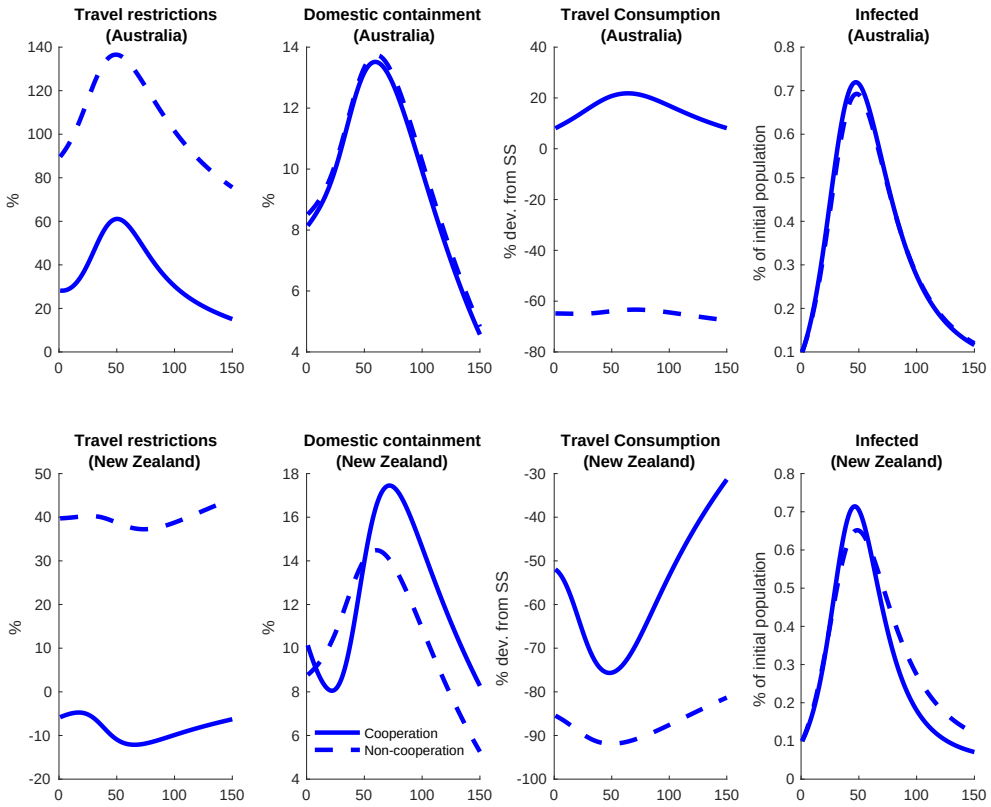

Figure 12: Cooperative and non-cooperative equilibrium for Australia and New Zealand.

is much higher, and travel consumption is much lower under the non-cooperative equilibrium than under the cooperative equilibrium. Domestic containment in Australia is very similar under the two regimes, while domestic containment in New Zealand is slightly higher under the non-cooperative equilibrium. For both regions, the infection curve under cooperation is just on top of that under non-cooperation, indicating that there is slightly more people infected under cooperation. Overall, there is a welfare gain from cooperation due to higher overall consumption.

We use the same method to calculate the value of travel bubble. The overall welfare gain of the travel bubble is valued at 307.8 USD per capita for the two countries. But the benefit is not evenly distributed between the two. Australia experiences a small loss of 412.3 USD per capita under the travel bubble, while New Zealand experiences a large gain of 5,347.4 USD per capita. As the share of New Zealanders' travel spending in Australia is much higher than that of Australians' travel spending in New Zealand, New Zealand benefits more from the less strict travel arrangement of the travel bubble. Interestingly, we see a travel subsidy implemented in New Zealand under cooperation. The sizable travel restriction in Australia under cooperation, however, shows that even under the travel bubble arrangement, a certain degree of travel restriction is still in place in the region with higher GDP and smaller travel openness as the economic benefit of traveling is relatively small.

7 Conclusion

Reopening borders has become a pressing issue as the world finds its way out from the COVID-19 pandemic. In this paper, we provide a framework for assessing various cross-border travel arrangements in a pandemic.

Using a two-region SIR-Macro model, we analyze the economic, health and overall welfare outcomes of a range of cooperative and non-cooperative travel arrangements. Our key finding is that cooperative travel arrangements improve the welfare for residents from non-cooperative arrangements. The improvement is Pareto optimal in a symmetric case. In cases when a region wishes to impose a border control, it is recommended that policy makers vaccinate the population in time before higher welfare costs are incurred. We find that with cooperative arrangements, pre-departure tests further improves the welfare.

Applying the model to real-life examples, we find that uneven relative demands for bilateral travel and GDP volumes between the regions may lead to non-Pareto outcome. This means that one region enjoys higher welfare while the other region experiences a loss, despite the overall welfare gain. Such an uneven welfare outcome is found in both travel arrangements between Singapore and Hong Kong, and between Australia and New Zealand, but it is closer to a Pareto outcome in the case between Singapore and Hong Kong. To compensate the loss in one region, further bargaining may be needed.

We leave several aspects for future research. These include labor market dynamics and other stimulus such as fiscal and monetary policies implemented in the regions.

A Data sources

A.1 Singapore – Hong Kong

We calibrate the model according to the bilateral tourism receipts and the private consumption expenditure of Singapore and Hong Kong. For the data, unless otherwise stated, the source is the CEIC Database. The total revenue for Hong Kong tourism was US$38175.375bn in 2017, with total tourist arrival of 58.47 million (XinhuaNet, 2018; Hong Kong Tourism Board, 2018). The visitors arrival from Singapore was 627,612, so by proportion, the spending of tourists from Singapore in Hong Kong was around US$409.77mn in 2017. The spending of tourists from Hong Kong in Singapore was reported as SG$563.434mn in 2017, which was around US$426.26mn. The private consumption expenditure was US$133.477bn in Singapore and US$251.872bn in Hong Kong in 2019. We cannot find the data for bilateral travel spending between the two regions in 2019, so we assume the travel spending was similar between 2017 and 2019. Thus, the share of tourism spending from Singapore spent in Hong Kong was around 0.307 percent, and the share of tourism spending from Hong Kong spent in Singapore was around 0.169 percent in 2019.

A.2 Australia – New Zealand

We calibrate the model according to the bilateral tourism receipts and the private consumption expenditure of Australia and New Zealand. For the data, unless otherwise stated, the source is the CEIC Database. The spending of tourists from New Zealand in Australia was AU$2.6bn in 2019, which was around US$1.965bn (Budget Direct, 2020). The private consumption expenditure in New Zealand was US$121.266bn in 2019. Thus, the share of tourism spending from New Zealand spent in Australia was around 1.620 percent in 2019.

The spending of tourists from Australia in New Zealand was NZ$2.7bn in 2019, which is around US$1.961bn (Tourism New Zealand, 2020). The private consumption expenditure in Australia was US$760.977bn in 2019. Thus, the share of tourism spending from Australia spent in New Zealand was around 0.258 percent in 2019.

B Model equations

B.1 Residents in H

The following 24 equations pin down the dynamics of U_t^s, U_t^i, U_t^r, C_t^s, C_t^i, C_t^r, C_{Ht}^s, C_{Ht}^i, C_{Ht}^r, C_{Ft}^s, C_{Ft}^i, C_{Ft}^r, N_t^s, N_t^i, N_t^r, C_t, N_t, $\lambda_{\tau t}$, Γ_t, τ_t, T_t, S_t, $\hat{I}_t$, R_t, given the paths of all variables for residents in F (with asterisks) and the policy variables ρ_t and μ_t.

- Recovered people

$$U_t^r = u\left(C_t^r, N_t^r\right) + \beta E_t U_{t+1}^r \tag{12}$$

$$\left(1+\rho_t\right) C_{Ht}^r + \left(1+\rho_t^*\right)\left(1+\mu_t^*\right) C_{Ft}^r = AN_t^r + A\Gamma_t \tag{13}$$

$$C_t{}^r = \left[(1-\upsilon)^{1/\eta}\, C_{Ht}{}^{r\,1-1/\eta} + \upsilon^{1/\eta} C_{Ft}{}^{r\,1-1/\eta}\right]^{\frac{\eta}{\eta-1}} \tag{14}$$

$$\left(1+\rho_t\right)\frac{\theta N_t^r}{A} = (1-\upsilon)^{1/\eta}\left(\frac{C_{Ht}^r}{C_t^r}\right)^{-1/\eta}\frac{1}{C_t^r} \tag{15}$$

$$\left(1+\rho_t^*\right)\left(1+\mu_t^*\right)\frac{\theta N_t^r}{A} = \upsilon^{1/\eta}\left(\frac{C_{Ft}^r}{C_t^r}\right)^{-1/\eta}\frac{1}{C_t^r} \tag{16}$$

- Infected people

$$U_t^i = u\left(C_t^i, N_t^i\right) + \beta E_t\left[\pi_r U_{t+1}^r + (1-\pi_r-\pi_d) U_{t+1}^i\right] \tag{17}$$

$$\left(1+\rho_t\right) C_{Ht}^i + \left(1+\rho_t^*\right)\left(1+\mu_t^*\right) C_{Ft}^i = AN_t^i + A\Gamma_t \tag{18}$$

$$C_t{}^i = \left[(1-\upsilon)^{1/\eta}\, C_{Ht}{}^{i\,1-1/\eta} + \upsilon^{1/\eta} C_{Ft}{}^{i\,1-1/\eta}\right]^{\frac{\eta}{\eta-1}} \tag{19}$$

$$\left(1+\rho_t\right)\frac{\theta N_t^i}{A} = (1-\upsilon)^{1/\eta}\left(\frac{C_{Ht}^i}{C_t^i}\right)^{-1/\eta}\frac{1}{C_t^i} \tag{20}$$

$$\left(1+\rho_t^*\right)\left(1+\mu_t^*\right)\frac{\theta N_t^i}{A} = \upsilon^{1/\eta}\left(\frac{C_{Ft}^i}{C_t^i}\right)^{-1/\eta}\frac{1}{C_t^i} \tag{21}$$

- Susceptible people

$$\tau_t = \pi_s C_{Ht}^s(\hat{I}_t C_{Ht}^i + \hat{I}_t^* C_{Ht}^{i*}) + \pi_s^* C_{Ft}^s(\hat{I}_t C_{Ft}^i + \hat{I}_t^* C_{Ft}^{i*}) \tag{22}$$

$$U_t^s = u(C_t^s, N_t^s) + \beta E_t\left[\tau_t U_{t+1}^i + (1-\tau_t) U_{t+1}^s\right] \tag{23}$$

$$\left(1+\rho_t\right) C_{Ht}^s + \left(1+\rho_t^*\right)\left(1+\mu_t^*\right) C_{Ft}^s = AN_t^s + A\Gamma_t \tag{24}$$

$$C_t^s = \left[(1-\upsilon)^{1/\eta}\, C_{Ht}^{s\,1-1/\eta} + \upsilon^{1/\eta} C_{Ft}^{s\,1-1/\eta}\right]^{\frac{\eta}{\eta-1}} \tag{25}$$

$$\left(1+\rho_t\right)\frac{\theta N_t^s}{A} = (1-\upsilon)^{1/\eta}\left(\frac{C_{Ht}^s}{C_t^s}\right)^{-1/\eta}\frac{1}{C_t^s} + \lambda_{\tau t}\pi_s\left(\hat{I}_t C_{Ht}^i + \hat{I}_t^* C_{Ht}^{i*}\right) \tag{26}$$

$$\left(1+\rho_t^*\right)\left(1+\mu_t^*\right)\frac{\theta N_t^s}{A} = \upsilon^{1/\eta}\left(\frac{C_{Ft}^s}{C_t^s}\right)^{-1/\eta}\frac{1}{C_t^s} + \lambda_{\tau t}\pi_s^*\left(\hat{I}_t C_{Ft}^i + \hat{I}_t^* C_{Ft}^{i*}\right) \tag{27}$$

$$\lambda_{\tau t} = \beta E_t\left(U_{t+1}^i - U_{t+1}^s\right) \tag{28}$$

- Population dynamics

$$T_t = \tau_t S_t \tag{29}$$
$$S_{t+1} = S_t - T_t \tag{30}$$
$$\hat{I}_{t+1} = \hat{I}_t + \frac{T_t}{pop_0} - (\pi_r + \pi_d)\hat{I}_t \tag{31}$$
$$R_{t+1} = R_t + \pi_r \hat{I}_t pop_0 \tag{32}$$

- Government budget

$$\left(S_t + \hat{I}_t pop_0 + R_t\right) A\Gamma_t = \rho_t \left(S_t C^s_{Ht} + \hat{I}_t pop_0 C^i_{Ht} + R_t C^r_{Ht}\right) + (\rho_t + \mu_t + \rho_t\mu_t) \left(S^*_t C^{s*}_{Ht} + \hat{I}^*_t pop^*_0 C^{i*}_{Ht} + R^*_t C^{r*}_{Ht}\right) \tag{33}$$

- Aggregation

$$C_t = S_t C^s_t + \hat{I}_t pop_0 C^i_t + R_t C^r_t \tag{34}$$
$$N_t = S_t N^s_t + \hat{I}_t pop_0 N^i_t + R_t N^r_t \tag{35}$$

B.2 Residents in F

The following 24 equations pin down the dynamics of U^{s*}_t, U^{i*}_t, U^{r*}_t, C^{s*}_t, C^{i*}_t, C^{r*}_t, C^{s*}_{Ft}, C^{i*}_{Ft}, C^{r*}_{Ft}, C^{s*}_{Ht}, C^{i*}_{Ht}, C^{r*}_{Ht}, N^{s*}_t, N^{i*}_t, N^{r*}_t, C^*_t, N^*_t, $\lambda^*_{\tau t}$, Γ^*_t, τ^*_t, T^*_t, S^*_t, $\hat{I}^*_t$, R^*_t, given the paths of all variables for residents in H (without asterisks) and the policy variables ρ^*_t and μ^*_t.

- Recovered people

$$U^{r*}_t = u\left(C^{r*}_t, N^{r*}_t\right) + \beta E_t U^{r*}_{t+1} \tag{36}$$
$$(1+\rho^*_t)\, C^{r*}_{Ft} + (1+\rho_t)(1+\mu_t)\, C^{r*}_{Ht} = AN^{r*}_t + A\Gamma^*_t \tag{37}$$
$$C^{*r}_t = \left[(1-\upsilon)^{1/\eta} C^{r*\,1-1/\eta}_{Ft} + \upsilon^{1/\eta} C^{r*\,1-1/\eta}_{Ht}\right]^{\frac{\eta}{\eta-1}} \tag{38}$$
$$(1+\rho^*_t)\frac{\theta N^{r*}_t}{A} = (1-\upsilon)^{1/\eta}\left(\frac{C^{r*}_{Ft}}{C^{r*}_t}\right)^{-1/\eta}\frac{1}{C^{r*}_t} \tag{39}$$
$$(1+\rho_t)(1+\mu_t)\frac{\theta N^{r*}_t}{A} = \upsilon^{1/\eta}\left(\frac{C^{r*}_{Ht}}{C^{r*}_t}\right)^{-1/\eta}\frac{1}{C^{r*}_t} \tag{40}$$

- Infected people

$$U_t^{i*} = u\left(C_t^{i*}, N_t^{i*}\right) + \beta E_t\left[\pi_r U_{t+1}^{r*} + (1-\pi_r-\pi_d)U_{t+1}^{i*}\right] \tag{41}$$

$$(1+\rho_t^*)\, C_{Ft}^{i*} + (1+\rho_t)\,(1+\mu_t)\, C_{Ht}^{i*} = AN_t^{i*} + A\Gamma_t^* \tag{42}$$

$$C_t^{*i} = \left[(1-\upsilon)^{1/\eta}\, C_{Ft}^{i*\,1-1/\eta} + \upsilon^{1/\eta} C_{Ht}^{i*\,1-1/\eta}\right]^{\frac{\eta}{\eta-1}} \tag{43}$$

$$(1+\rho_t^*)\,\frac{\theta N_t^{i*}}{A} = (1-\upsilon)^{1/\eta}\left(\frac{C_{Ft}^{i*}}{C_t^{i*}}\right)^{-1/\eta}\frac{1}{C_t^{i*}} \tag{44}$$

$$(1+\rho_t)\,(1+\mu_t)\,\frac{\theta N_t^{i*}}{A} = \upsilon^{1/\eta}\left(\frac{C_{Ht}^{i*}}{C_t^{i*}}\right)^{-1/\eta}\frac{1}{C_t^{i*}} \tag{45}$$

- Susceptible people

$$\tau_t^* = \pi_s^* C_{Ft}^{s*}(\hat{I}_t^* C_{Ft}^{i*} + \hat{I}_t C_{Ft}^{i}) + \pi_s C_{Ht}^{s*}(\hat{I}_t^* C_{Ht}^{i*} + \hat{I}_t C_{Ft}^{i*}) \tag{46}$$

$$U_t^{s*} = u(C_t^{s*}, N_t^{s*}) + \beta E_t\left[\tau_t^* U_{t+1}^{i*} + (1-\tau_t^*)U_{t+1}^{s*}\right] \tag{47}$$

$$(1+\rho_t^*)\, C_{Ft}^{s*} + (1+\rho_t)\,(1+\mu_t)\, C_{Ht}^{s*} = AN_t^{s*} + A\Gamma_t^* \tag{48}$$

$$C_t^{s*} = \left[(1-\upsilon)^{1/\eta}\, C_{Ft}^{s*\,1-1/\eta} + \upsilon^{1/\eta} C_{Ht}^{s*\,1-1/\eta}\right]^{\frac{\eta}{\eta-1}} \tag{49}$$

$$(1+\rho_t^*)\frac{\theta N_t^{s*}}{A} = (1-\upsilon)^{1/\eta}\left(\frac{C_{Ft}^{s*}}{C_t^{s*}}\right)^{-1/\eta}\frac{1}{C_t^{s*}} + \lambda_{\tau t}^*\pi_s^*\left(\hat{I}_t^* C_{Ft}^{i*} + \hat{I}_t C_{Ft}^{i}\right) \tag{50}$$

$$(1+\rho_t)\,(1+\mu_t)\,\frac{\theta N_t^{s*}}{A} = \upsilon^{1/\eta}\left(\frac{C_{Ht}^{s*}}{C_t^{s*}}\right)^{-1/\eta}\frac{1}{C_t^{s*}} + \lambda_{\tau t}^*\pi_s\left(\hat{I}_t^* C_{Ht}^{i*} + \hat{I}_t C_{Ht}^{i}\right) \tag{51}$$

$$\lambda_{\tau t}^* = \beta E_t\left(U_{t+1}^{i*} - U_{t+1}^{s*}\right) \tag{52}$$

- Population dynamics

$$T_t^* = \tau_t^* S_t^* \tag{53}$$

$$S_{t+1}^* = S_t^* - T_t^* \tag{54}$$

$$\hat{I}_{t+1}^* = \hat{I}_t^* + \frac{T_t^*}{pop_0^*} - (\pi_r+\pi_d)\hat{I}_t^* \tag{55}$$

$$R_{t+1} = R_t + \pi_r \hat{I}_t^* pop_0^* \tag{56}$$

- Government budget

$$\left(S_t^* + \hat{I}_t^* pop_0^* + R_t^*\right) A\Gamma_t^* = \rho_t^*\left(S_t^* C_{Ft}^{s*} + \hat{I}_t^* pop_0^* C_{Ft}^{i*} + R_t^* C_{Ft}^{r*}\right) + (\rho_t^* + \mu_t^* + \rho_t^*\mu_t^*)\left(S_t C_{Ft}^{s} + \hat{I}_t pop_0 C_{Ft}^{i} + R_t C_{Ft}^{r}\right) \tag{57}$$

- Aggregation

$$C_t^* = S_t^* C_t^{s*} + \hat{I}_t^* pop_0^* C_t^{i*} + R_t^* C_t^{r*} \tag{58}$$

$$N_t^* = S_t^* N_t^{s*} + \hat{I}_t^* pop_0^* N_t^{i*} + R_t^* N_t^{r*} \tag{59}$$

References

Acemoglu, D., V. Chernozhukov, I. Werning, and M. Whinston (2020, May). Optimal targeted lockdowns in a multi-group sir model. Draft.

Alvarez, F., D. Argente, and F. Lippi (2020, April). A simple planning problem for covid-19 lockdown. Draft, University of Chicago.

Australian Government Department of Home Affairs (2021, June). New zealand safe travel zone. Australian Government Department of Home Affairs.

BBC (2020, November). Covid-19: Hong Kong-Singapore travel corridor postponed. *BBC News*.

Benigno, G. and P. Benigno (2006, April). Designing targeting rules for international monetary policy cooperation. *Journal of Monetary Economics 53*(3), 473–506.

Bodenstein, M., L. Guerrieri, and J. LaBriola (2019, January). Macroeconomic policy games. *Journal of Monetary Economics 101*, 64–81.

Brotherhood, L., P. Kircher, C. Santos, and M. Tertilt (2020, May). An economic model of the covid-19 epidemic: The importance of testing and age-specific policies. Draft.

Budget Direct (2020, June). Australian tourism statistics 2020. Budget Direct.

ChannelNewsAsia (2021a, May). COVID-19: Singapore-Hong Kong air travel bubble to be deferred for a second time.

ChannelNewsAsia (2021b, April). Singapore, Hong Kong to relaunch travel bubble on May 26. ChannelNewsAsia.

Clarida, R., J. Gali, and M. Gertler (2002, July). A simple framework for international monetary policy analysis. *Journal of Monetary Economics 49*(5), 879–904.

CNN (2020, November). Hong Kong and Singapore confirm date for launch of new 'travel bubble'.

Corsetti, G. and P. Pesenti (2001, May). Welfare and Macroeconomic Interdependence*. *The Quarterly Journal of Economics 116*(2), 421–445.

Corsetti, G. and P. Pesenti (2005, March). International dimensions of optimal monetary policy. *Journal of Monetary Economics 52*(2), 281–305.

Eichenbaum, M. S., S. Rebelo, and M. Trabandt (2021, April). The Macroeconomics of Epidemics. *The Review of Financial Studies* (hhab040).

Engel, C. (2011, October). Currency Misalignments and Optimal Monetary Policy: A Reexamination. *American Economic Review 101*(6), 2796–2822.

Fujiwara, I. and J. Wang (2017, September). Optimal monetary policy in open economies revisited. *Journal of International Economics 108*, 300–314.

George, A., C. Li, J. Z. Lim, and T. Xie (2021, August). From SARS to COVID-19: The evolving role of China-ASEAN production network. *Economic Modelling 101*, 105510.

Giannone, E., N. Paixão, and X. Pang (2020, October). The geography of pandemic containment. *COVID Economics* (52), 68–95.

Glover, A., J. Heathcote, D. Krüger, and J.-V. Rios-Rull (2020, March). Health versus wealth: On the distributional effects of controlling a pandemic. Draft.

Guerrieri, V., G. Lorenzoni, L. Straub, and I. Werning (2020, March). Macroeconomic implications of covid-19: Can negative supply shocks cause demand shortages? Draft, MIT.

HKSAR (2021, June). Target date of inaugural flights under HK-Singapore Air Travel Bubble to be reviewed in early July. Governments of the Hong Kong Special Administrative Region (HKSAR).

Hong Kong Tourism Board (2018). Best of all, it's in Hong Kong – Hong Kong Tourism Board Annual Report 2017/18. Technical report.

Hou, X., S. Gao, Q. Li, Y. Kang, N. Chen, K. Chen, J. Rao, J. S. Ellenberg, and J. A. Patz (2021, June). Intracounty modeling of COVID-19 infection with human mobility: Assessing spatial heterogeneity with business traffic, age, and race. *Proceedings of the National Academy of Sciences 118*(24). Publisher: National Academy of Sciences Section: Social Sciences.

Hsu, W.-T., H.-C. L. Lin, and Y. Han (2020). Between Lives and Economy: Optimal COVID-19 Containment Policy in Open Economies.

Krueger, D., H. Uhlig, and T. Xie (2020, April). Macroeconomic Dynamics and Reallocation in an Epidemic. Working Paper 27047, National Bureau of Economic Research. Series: Working Paper Series.

NZ Herald (2020, December). Travel bubble with australia could be early next year - pm. NZ Herald.

Obstfeld, M. and K. Rogoff (1995). Exchange Rate Dynamics Redux. *Journal of Political Economy 103*(3), 624–660.

Obstfeld, M. and K. Rogoff (2002, May). Global Implications of Self-Oriented National Monetary Rules*. *The Quarterly Journal of Economics 117*(2), 503–535.

Tourism New Zealand (2020). Markets & stats australia overview. Tourism New Zealand.

XinhuaNet (2018, January). Hong Kong tourist arrivals up 3.2 pct in 2017 - Xinhua | English.news.cn. XinhuaNet.